



Shahid Chamran  
University of Ahvaz

# Journal of Applied and Computational Mechanics



Research Paper

## Analysis of Free Vibration of Porous Power-law and Sigmoid Functionally Graded Sandwich Plates by the R-functions Method

Lidiya Kurpa<sup>1</sup>, Tetyana Shmatko<sup>2</sup>, Jan Awrejcewicz<sup>3</sup>, Galina Timchenko<sup>1</sup>, Iryna Morachkovska<sup>1</sup>

<sup>1</sup> Department of Applied Mathematics, National Technical University "Kharkiv Polytechnic Institute",  
Kharkiv, Ukraine, Email: kurpalidia@gmail.com (K.L.); gntimchenko2000@gmail.com (G.T.); i.morachkovska@gmail.com (I.M.)

<sup>2</sup> Department of Higher Mathematics, National Technical University "Kharkiv Polytechnic Institute", Kharkiv, Ukraine, Email: ktv\_ua@yahoo.com

<sup>3</sup> Department of Automation, Biomechanical and Mechatronics, Lodz University of Technology, Lodz, Poland, Email: jan.awrejcewicz@p.lodz.pl

Received April 11 2023; Revised June 26 2023; Accepted for publication July 14 2023.

Corresponding author: G. Timchenko (gntimchenko2000@gmail.com)

© 2023 Published by Shahid Chamran University of Ahvaz

**Abstract.** Investigation of free vibration of porous power and sigmoid-law sandwich functionally graded (FG) plates with different boundary conditions is presented in this paper. The FG sandwich plate includes three layers. The face layers are fabricated of functionally graded material (FGM) and middle layer (core) is isotropic (ceramic). Imperfect sigmoid FG sandwich plates with even and linear-uneven porosities and nonporous core layer are studied. Developed approach has been realized in the framework of a refined theory of the first-order shear deformation theory (FSDT) using variational methods and the R-functions theory. The analytical expressions are obtained for calculating the elastic characteristics with the assumption that the values of Poisson's ratio are the same for constituent FGM materials. For rectangular plates, the obtained results are compared with known results and a good agreement is obtained. Vibration analysis of a complex-shaped porous sandwich plate made of FGM has been performed. The effect of various parameters on the dynamic behavior of the plate, such as the type and values of porosity coefficients, power index, lay-up scheme, types of FGM, has been studied.

**Keywords:** Power-law, sigmoid-law, porosity, free vibration, functionally graded sandwich plates, the R-functions theory, variational Ritz method.

### 1. Introduction

The study of the dynamic behavior of sandwich plates and shells made of functionally graded materials (FGM) attracts the attention of many researchers. This is due to the widespread use of FGM in many industries such as military, aviation and missile industries, shipbuilding, machine building and others. The most important properties of these materials are high strength and lightness, smooth and continuous transition in properties in one or more directions. These properties are especially important in the case of multilayer or sandwich plates and shells. Therefore, many scientists developed models and methods to investigate static and dynamic behavior of such objects. In particular, the study of FGM porous sandwich plates with different planform, boundary conditions, and constituents of the FGM, varied arrangement and thickness of the layers is an actual problem. A detailed review of the publications discussing the bending, vibration and stability of the FGM sandwich plates and shells is presented in papers [1-4] and others. Many theories and methods have been developed to investigate the static and dynamic behavior of FGM plates and shells. We can name among them the method of Rayleigh-Ritz, Galerkin method, finite difference method, finite element method, differential quadrature and differential transformations methods, boundary integral equations method, collocation method, etc.

To study vibration of the FGM sandwich plates, the higher-order shear deformation theory (HSDT) and many of its modifications are used [5-12]. It is important that these theories do not require shear correction factor. The first-order shear deformation theory (FSDT) is the simplest and it gives acceptable results for moderately thick plates, so a lot of scientists have used this theory to study the vibrations of FG plates [13-17]. One of the disadvantages of this theory is a difficulty in determining the shear correction factor, which depends on material, plate geometry, boundary conditions, etc. That is why some approaches were proposed to improve the accuracy and efficiency of this theory. In papers [4, 13], it was proposed to improve the FSDT by introducing a new shear distributed function. Due to a certain choice of this function, the shear strain changes according to the parabolic law over the thickness and equals zero on the face surfaces. Thai et al. [15, 16] improved the FSDT by division of the transverse displacement into bending and shear part. Modified FSDT was considered by Amabili [17] to research the nonlinear vibration and stability of the laminated shells. To analyze the bending and free vibration of FG plates Tan-Van et al. [18] applied a simple FSDT combined with a mesh free method.

During the fabrication process of FGMs, such features as porosity often appear. The presence of porosity reduces the mass of the structures, and besides, the porosity distribution through the thickness can improve the strength of the structures. FG structures with porosity have been widely applied in many fields of engineering to reduce the weight of equipment and increase heat



resistance. That is why a lot of scientists have been focused on the investigation of the static and dynamic response of the sandwich FG plates with porosity. Let us analyze the works considering the vibration of the FGM porous sandwich plates. Vinh and Huy [19] presented some review of publications about this problem. Free vibration analysis of the porous rectangular plates was carried out in papers [19-23]. Vinh and Huy [19] developed a finite element model based on a new hyperbolic shear deformation theory. Numerical results for deflection, frequencies, critical loads of rectangular plates with different types of boundary conditions and different ways of porosity distribution are presented. Shamsavari et al. [20] developed a new quasi-3D hyperbolic theory for the free vibration of FG plates with porosities resting on elastic foundations. Zenkour [21] studied the bending responses of the FG porous single-layered and sandwich thick rectangular plates according to a quasi-3D shear deformation theory. Daikh and Zencour [22] analyzed the free vibration and buckling of porous FG sandwich rectangular simply supported plates. Simple higher-order shear deformation theory was suggested to solve this problem. There were considered four types of porosity distribution based on the sigmoid and power functions. Xiang et al. [23] studied the vibration of sandwich plate with functionally graded face and homogeneous core. Gupta and Talha [24] investigated the effect of porosity on the free vibration response of FGM plates in a thermal environment. Akbas [25] examined different mechanical behaviors of the FG porous plates, beams, and nanorods. Wu et al. [26] used finite element method to study the free and forced vibrations of the FG porous structures. Chen et al. [27] dealt with the buckling and bending of analyses of the FG porous plate using the Chebyshev-Ritz method. Rahmani et al. [28] investigated the vibration behavior of two types of porous FG circular sandwich plates applying a modified higher order sandwich plate theory. Zhang et al. [29] presented the free vibration and damping analysis of the FG porous sandwich plates based on a modified Fourier-Ritz method. To investigate the bending, free vibration, and buckling of the FGSPs plates. Hadji and Avcar [30] considered the square FG sandwich porous plates with various boundary conditions and three different types of porosity distribution using hyperbolic shear displacement theory. Authors of the papers [31, 32] studied free vibrations of the imperfect FGM sandwich plates on two parameters elastic foundation. Hadji and Avcar et al. [31] have applied third shear deformation theory (TSDT). They have obtained analytical solution for simply supported square plate and investigated effect of the different mechanical parameters on fundamental frequency. Sobhani and Avcar [32] have explored imperfect graphene nanoplatelet reinforced nanocomposite conical and cylindrical shell, and also annular plate resting on Winkler-Pasternak foundations. To formulate the problem, the authors used FSDT. Discretization of the motion equations was carried out using Generalized Differential Quadrature Method.

By the literature reviewed, the authors made the following conclusion. A lot of research papers are available on the vibration and static analysis of the FGM sandwich plates. However, literature on FG sandwich porous plate is limited. Simply supported rectangular plate is mostly studied. Especially, the authors have not found any paper where plates with an arbitrary planform and different boundary conditions were analyzed.

In this work, we propose to use the variational Rayleigh-Ritz method together with the R-functions theory (RFM) [33, 34]. This is a numerical-analytical method that allows one to construct the systems of the admissible functions that satisfy all or only kinematic boundary conditions, including mixed ones in case of an arbitrary shape of the plate. As a result, a desired solution is presented in an analytical form. This result is significant for a solution of nonlinear vibration problems.

Earlier, RFM was applied to solve many actual problems [35-42] connected with the vibration and stability of the FGM perfect plates and shallow shells. In this paper, RFM is used for the first time to study vibration of FG sandwich porous plates with an arbitrary planform, power-law, and sigmoid porosities distribution. The first-order shear deformation theory is applied with given shear cofactor.

### 2. Mathematical Formulation of the Problem

We consider a sandwich plate with an arbitrary planform as shown in Fig. 1. It is assumed that plate consists of three layers. The upper and lower (face) layers are fabricated from functionally graded materials (FGM) and middle layer (core) is isotropic. The face layers are graded from metal to ceramic. The core is made of ceramic.

Volume fraction  $V^{(n)}(z)$ , ( $n = 1,2,3$ ) for power-law (P-law) can be defined as [22]:

$$\begin{cases} V^{(1)}(z) = \left(\frac{z + \frac{h}{2}}{h_1 + \frac{h}{2}}\right)^p, & -\frac{h}{2} \leq z \leq h_1, \\ V^{(2)}(z) = 1, & h_1 \leq z \leq h_2, \\ V^{(3)}(z) = \left(\frac{z - \frac{h}{2}}{h_2 - \frac{h}{2}}\right)^p, & h_2 \leq z \leq \frac{h}{2}. \end{cases} \tag{1}$$

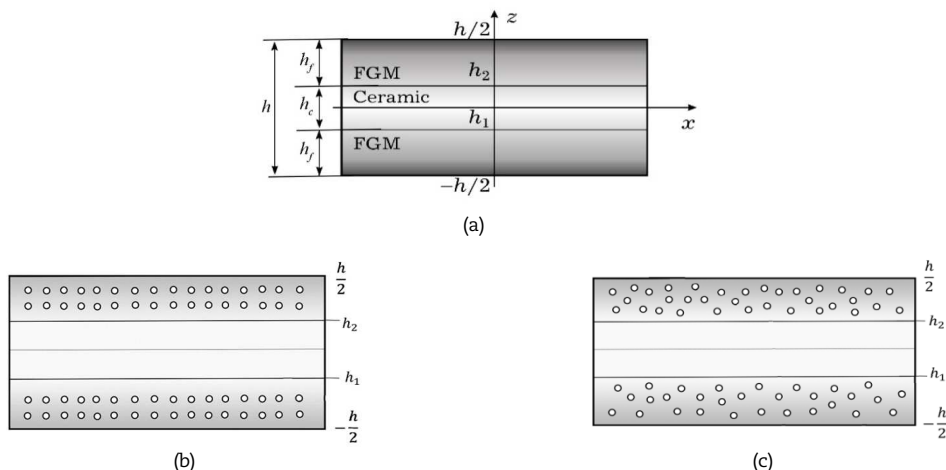


Fig. 1. (a) The structure of functionally graded sandwich plate with (b) even and (c) linear-uneven porosity distributions.



Volume fraction of the layers for sigmoid-law (S-law) can be expressed as [22]:

$$\begin{cases} V^{(1)}(z) = \frac{1}{2} \left( \frac{z + \frac{h}{2}}{h_m + \frac{h}{2}} \right)^p, & -\frac{h}{2} \leq z \leq h_m, \\ V^{(1)}(z) = 1 - \frac{1}{2} \left( \frac{z - h_1}{h_m + h_1} \right)^p, & h_m \leq z \leq h_1, \\ V^{(2)}(z) = 1 & h_1 \leq z \leq h_2, \\ V^{(3)}(z) = 1 - \frac{1}{2} \left( \frac{z - h_2}{h_n + h_2} \right)^p, & h_2 \leq z \leq h_n, \\ V^{(3)}(z) = \frac{1}{2} \left( \frac{z - \frac{h}{2}}{h_n - \frac{h}{2}} \right)^p, & h_n \leq z \leq \frac{h}{2}. \end{cases} \tag{2}$$

The values  $h_m$  and  $h_n$  denote the middle of the lower and upper layers respectively and have the following form:

$$h_m = \frac{1}{2} \left( h_1 - \frac{h}{2} \right), \quad h_n = \frac{1}{2} \left( h_2 + \frac{h}{2} \right).$$

In this study, the effective material properties of FGMs are calculated for two models of the porosity distribution (even and linear- uneven) [22], which are independent for each layer.

The effective material properties for imperfect FGM with even porosities are defined as:

$$\begin{cases} P^{(1)}(z) = P_m + (P_c - P_m)V^{(1)}(z) - \frac{\alpha}{2}(P_c + P_m), \\ P^{(2)}(z) = P_m + (P_c - P_m)V^{(2)}(z), \\ P^{(3)}(z) = P_m + (P_c - P_m)V^{(3)}(z) - \frac{\alpha}{2}(P_c + P_m). \end{cases} \tag{3}$$

The effective material properties for imperfect FGM with linear-uneven porosities are defined as:

$$\begin{cases} P^{(1)}(z) = P_m + (P_c - P_m)V^{(1)}(z) - \frac{\alpha}{2}(P_c + P_m) \left( 1 + \frac{z - h_1}{\frac{h}{2} + h_1} \right), \\ P^{(2)}(z) = P_m + (P_c - P_m)V^{(2)}(z), \\ P^{(3)}(z) = P_m + (P_c - P_m)V^{(3)}(z) - \frac{\alpha}{2}(P_c + P_m) \left( \frac{z - \frac{h}{2}}{h_2 - \frac{h}{2}} \right). \end{cases} \tag{4}$$

By FSDT [16, 43], the displacements  $u, v, w$  at any point in the plate are expressed as functions of the middle surface displacements  $u_0, v_0$  and  $w$  in the  $Ox, Oy$  and  $Oz$  directions and the independent rotations  $\psi_x, \psi_y$  of the transverse normal to middle surface about the  $Oy$  and  $Ox$  axes, respectively:

$$\begin{aligned} u(x, y, z, t) &= u_0(x, y, t) + z\psi_x(x, y, t), \\ v(x, y, z, t) &= v_0(x, y, t) + z\psi_y(x, y, t), \\ w(x, y, z, t) &= w_0(x, y, t). \end{aligned} \tag{5}$$

The strain components  $\{\varepsilon\} = \{\varepsilon_{11}, \varepsilon_{22}, \varepsilon_{12}\}^T$  and  $\{\gamma_0\} = \{\varepsilon_{13}, \varepsilon_{23}\}^T$  are expressed as  $\{\varepsilon\} = \{\varepsilon_0\} + z\{\chi\}$ , where:

$$\{\varepsilon_0\} = \{u_{0,x}, \quad v_{0,y}, \quad u_{0,y} + v_{0,x}\}^T, \tag{6}$$

$$\{\chi\} = \{\phi_{x,x}, \quad \phi_{y,y}, \quad \phi_{x,y} + \phi_{y,x}\}^T. \tag{7}$$

Comma defines the differentiation of the function with respect to argument that follows for it.

The total in plane resultant force  $N = (N_{11}, N_{22}, N_{12})^T$ , the total resultant moment  $M = (M_{11}, M_{22}, M_{12})^T$  and the transverse force resultants  $Q = (Q_x, Q_y)^T$  are given by:

$$\{N\} = [A]\{\varepsilon\} + [B]\{\chi\}, \quad \{M\} = [B]\{\varepsilon\} + [D]\{\chi\}, \quad \{Q\} = K_s^2 A_{66} \{\varepsilon_{13}, \varepsilon_{23}\}^T, \tag{8}$$

where  $K_s^2$  denotes the shear correction factor. In this paper, we take  $K_s^2=5/6$ . Note that the elements  $A_{ij}, B_{ij}, D_{ij}$  of the matrices  $[A], [B]$  and  $[D]$  in relations (8) are calculated by:

$$A_{ij} = \sum_{r=1}^3 \int_{z_r}^{z_{r+1}} Q_{ij}^{(r)} dz, \quad B_{ij} = \sum_{r=1}^3 \int_{z_r}^{z_{r+1}} Q_{ij}^{(r)} z dz, \quad D_{ij} = \sum_{r=1}^3 \int_{z_r}^{z_{r+1}} Q_{ij}^{(r)} z^2 dz, \tag{9}$$

where  $z_1 = -h/2, z_2 = h_1, z_3 = h_2, z_4 = h/2$ . The general thickness  $h$  is a constant value. The values  $h_1$  and  $h_2$  determine the position of the lower and upper borders of the middle layer (core). The values  $Q_{ij}^{(r)}(i, j = 1, 2, 6)$  are defined by the following expressions:

$$Q_{11}^{(r)} = Q_{22}^{(r)} = \frac{E^{(r)}}{1 - (\nu^{(r)})^2}, \quad Q_{12}^{(r)} = \frac{\nu^{(r)} E^{(r)}}{1 - (\nu^{(r)})^2}, \quad Q_{66}^{(r)} = \frac{E^{(r)}}{2(1 + \nu^{(r)})}. \tag{10}$$

Here,  $E^{(r)}, \nu^{(r)}$  are the Young's modulus and Poisson's ratio of the corresponding layer, respectively.

Let us present the analytical expression of elements  $A_{ij}, B_{ij}, D_{ij}$  for two cases of the porosity distribution. For a short record, we introduce the following auxiliary designations:

$$E_{cm} = E_c - E_m, \quad E_{cm}^{(s)} = \alpha \frac{E_c + E_m}{2}, \quad h_c = h_2 - h_1, \quad AS1 = h_1 + \frac{h}{2}, \quad AS2 = h_2 - \frac{h}{2}.$$



Then, the following analytical expressions can be presented:

$$A_{11}^{(1,2)} = \frac{1}{1-\nu^2} (A_{11}^{(com)} - E_{cm}^{(s)} P_{11}^{(1,2)}), \quad B_{11}^{(1,2)} = \frac{1}{1-\nu^2} (B_{11}^{(com)} - E_{cm}^{(s)} P_{12}^{(1,2)}), \quad D_{11}^{(1,2)} = \frac{1}{1-\nu^2} (D_{11}^{(com)} - E_{cm}^{(s)} P_{13}^{(1,2)}). \quad (11)$$

Here, the superscripts, (1,2) correspond to even (1) and linear-uneven (2) distribution of porosity. The expressions  $A_{11}^{(com)}$ ,  $B_{11}^{(com)}$ ,  $D_{11}^{(com)}$  are defined by different formulas for P-law and S-law porosity distributions as:

**P-law:**

$$A_{11}^{(com)} = A_{11}^{(gP)}, \quad B_{11}^{(com)} = B_{11}^{(gP)}, \quad D_{11}^{(com)} = D_{11}^{(gP)}.$$

where,

$$A_{11}^{(gP)} = E_m h + E_{cm} \left( \frac{h+p h_c}{p+1} \right), \quad B_{11}^{(gP)} = E_{cm} \left( \frac{h_2^2 - h_1^2}{2} + \frac{AS1^2 - AS2^2}{p+2} - \frac{h(AS1 + AS2)}{2(p+1)} \right), \quad (12)$$

$$D_{11}^{(gP)} = E_m \frac{h^3}{12} + E_{cm} \left( \frac{AS1^3 - AS2^3}{p+3} - \frac{h(AS1^2 + AS2^2)}{p+2} + \frac{h_2(AS1 - AS2)}{4(p+1)} + \frac{h_2^3 - h_1^3}{3} \right).$$

**S-law:**

$$A_{11}^{(com)} = A_{11}^{(gS)}, \quad B_{11}^{(com)} = B_{11}^{(gS)}, \quad D_{11}^{(com)} = D_{11}^{(gS)},$$

where  $A_{11}^{(gS)}$ ,  $B_{11}^{(gS)}$ ,  $D_{11}^{(gS)}$  are:

$$A_{11}^{(gS)} = E_m h + \frac{1}{2} E_{cm} (h + h_c), \quad B_{11}^{(gS)} = \frac{1}{2} E_{cm} (h_2^2 - h_1^2) + \frac{AS2^2 - AS1^2}{2(p+1)(p+2)}, \quad (13)$$

$$D_{11}^{(gS)} = E_m \frac{h^3}{12} + E_{cm} \left( \frac{h_2^3 - h_1^3}{3} + \frac{AS2^2 (h_2 + \frac{h}{2}) - AS1^2 (h_1 - \frac{h}{2})}{4(p+1)(p+2)} \right).$$

The coefficients  $P_{11}^{(1,2)}$ ,  $P_{12}^{(1,2)}$ ,  $P_{13}^{(1,2)}$  for P-law and S-law cases have the same form. Even distribution of the porosity takes the form:

$$P_{11}^{(1)} = (h - h_c), \quad P_{12}^{(1)} = \left( \frac{h_1^2 - h_2^2}{2} \right), \quad P_{13}^{(1)} = \left( \frac{h^3}{12} - \frac{h_2^3 - h_1^3}{3} \right), \quad (14)$$

The linear-uneven distribution of the porosity can be defined as:

$$P_{11}^{(2)} = \frac{1}{2} (h - h_c), \quad P_{12}^{(2)} = \left( \frac{AS1^2 - AS2^2}{3} - \frac{1}{4} h (h_1 + h_2) \right), \quad (15)$$

$$P_{13}^{(2)} = \left( \frac{1}{3} \left( \frac{h^3}{8} + h_1^3 \right) - \frac{AS1^3 + AS2^3}{4} + \frac{2h_1 AS1^2 - h AS2^2}{3} - \frac{1}{2} \left( AS1 h_1^2 + AS2 \frac{h^2}{4} \right) \right).$$

The values  $A_{12}$ ,  $A_{66}$ ,  $B_{12}$ ,  $B_{66}$ ,  $D_{12}$ ,  $D_{66}$  are defined as:

$$A_{12} = \nu A_{11}, \quad A_{22} = A_{11}, \quad A_{66} = \frac{1-\nu}{2} A_{11},$$

$$B_{12} = \nu B_{11}, \quad B_{22} = B_{11}, \quad B_{66} = \frac{1-\nu}{2} B_{11}, \quad (16)$$

$$D_{12} = \nu D_{11}, \quad D_{22} = D_{11}, \quad D_{66} = \frac{1-\nu}{2} D_{11}.$$

The equations of motions are presented below:

$$A_{11}(L_{11}u + L_{12}v) + B_{11}(L_{14}\psi_x + L_{15}\psi_y) = I_0 \frac{\partial^2 u}{\partial t^2} + I_1 \frac{\partial^2 \psi_x}{\partial t^2}, \quad (17)$$

$$A_{11}(L_{21}u + L_{22}v) + B_{11}(L_{24}\psi_x + L_{25}\psi_y) = I_0 \frac{\partial^2 v}{\partial t^2} + I_1 \frac{\partial^2 \psi_y}{\partial t^2}, \quad (18)$$

$$L_{33}w + L_{34}\psi_x + L_{35}\psi_y = I_0 \frac{\partial^2 w}{\partial t^2}, \quad (19)$$

$$B_{11}(L_{41}u + L_{42}v) + L_{43}w + (D_{11}L_{44} - K_s A_{66})\psi_x + (D_{11}L_{45} - K_s A_{66})\psi_y = I_1 \frac{\partial^2 u}{\partial t^2} + I_2 \frac{\partial^2 \psi_x}{\partial t^2}, \quad (20)$$

$$B_{11}(L_{51}u + L_{52}v) + L_{53}w + D_{11}L_{54}\psi_x + (D_{11}L_{55} - K_s A_{66})\psi_y = I_1 \frac{\partial^2 v}{\partial t^2} + I_2 \frac{\partial^2 \psi_y}{\partial t^2}. \quad (21)$$

The linear operators have the following forms:

$$L_{11} = L_{14} = L_{41} = L_{44} = \frac{1}{1-\nu^2} \frac{\partial^2}{\partial x^2} + \frac{1}{2(1+\nu)} \frac{\partial^2}{\partial y^2}, \quad (22)$$



$$L_{22} = L_{25} = L_{52} = L_{55} = \frac{1}{1-\nu^2} \frac{\partial^2}{\partial y^2} + \frac{1}{2(1+\nu)} \frac{\partial^2}{\partial x^2}, \quad L_{33} = K_s A_{66} \left( \frac{\partial^2}{\partial x^2} + \frac{\partial^2}{\partial y^2} \right), \tag{23}$$

$$L_{12} = L_{21} = L_{24} = L_{42} = L_{45} = L_{54} = L_{15} = L_{51} = \frac{1}{2(1-\nu)} \frac{\partial^2}{\partial x \partial y}, \tag{24}$$

$$L_{34} = K_s A_{66} \frac{\partial}{\partial x}, \quad L_{35} = K_s A_{66} \frac{\partial}{\partial y}, \quad L_{43} = -L_{34}, \quad L_{53} = -L_{35}. \tag{25}$$

The cofactors  $I_0, I_1, I_2$  in equations (17) to (21), are expressed by:

$$(I_0, I_1, I_2) = \sum_{r=1}^3 \int_{z_r}^{z_{r+1}} (\rho^{(r)})(1, z, z^2) dz. \tag{26}$$

The mass density  $\rho^{(r)}$  of the  $r$ -th layer is calculated by formulas (3) and (4). The expressions of the values  $I_0, I_1, I_2$  is carried out by the following analytical expressions:

**P-law:**

$$I_0^{(1,2)} = (IA_{11}^{(c0m)} - \rho_{cm}^{(s)} P_{11}^{(1,2)}), \quad I_1^{(1,2)} = (IB_{11}^{(com)} - \rho_{cm}^{(s)} P_{12}^{(1,2)}), \quad I_2^{(1,2)} = (ID_{11}^{(com)} - \rho_{cm}^{(s)} P_{13}^{(1,2)}), \tag{27}$$

where the expressions  $IA_{11}^{(com)}, IB_{11}^{(com)}, ID_{11}^{(com)}$  are defined as:

**P-law:**

$$IA_{11}^{(com)} = IA_{11}^{(gP)}, \quad IB_{11}^{(com)} = IB_{11}^{(gP)}, \quad ID_{11}^{(com)} = ID_{11}^{(gP)},$$

where,

$$IA_{11}^{(gP)} = \rho_m h + \rho_{cm} \left( \frac{h+p}{p+1} h_c \right),$$

$$IB_{11}^{(gP)} = \rho_{cm} \left( \frac{h_2^2 - h_1^2}{2} + \frac{AS1^2 - AS2^2}{p+2} - \frac{h(AS1 + AS2)}{2(p+1)} \right), \tag{28}$$

$$ID_{11}^{(gP)} = \rho_m \frac{h^3}{12} + \rho_{cm} \left( \frac{AS1^3 - AS2^3}{p+3} - \frac{h(AS1^2 + AS2^2)}{p+2} + \frac{h_2(AS1 - AS2)}{4(p+1)} + \frac{h_2^3 - h_1^3}{3} \right).$$

**S-law:**

$$IA_{11}^{(com)} = IA_{11}^{(gS)}, \quad IB_{11}^{(com)} = IB_{11}^{(gS)}, \quad ID_{11}^{(com)} = ID_{11}^{(gS)}.$$

where the terms  $IA_{11}^{(gS)}, IB_{11}^{(gS)}, ID_{11}^{(gS)}$  are described as:

$$IA_{11}^{(gS)} = \rho_m h + \frac{1}{2} \rho_{cm} (h + h_c), \quad IB_{11}^{(gS)} = \frac{1}{2} \rho_{cm} (h_n^2 - h_m^2) + \frac{AS2^2 - AS1^2}{2(p+1)(p+2)}, \tag{29}$$

$$ID_{11}^{(gS)} = \rho_m \frac{h^3}{12} + \rho_{cm} \left( \frac{h_n^3 - h_m^3}{3} + \frac{AS2^2 (h_2 + \frac{h}{2}) - AS1^2 (h_1 - \frac{h}{2})}{4(p+1)(p+2)} \right).$$

The expressions  $P_{11}^{(1,2)}, P_{12}^{(1,2)}, P_{13}^{(1,2)}$  in formulas (27) have the form (14) and (15).

### 3. Method of Solution

It is known that the Rayleigh-Ritz method is one of the effective methods for solving problems of vibrations of plates and shells. However, the construction of admissible functions is a main difficulty that arises when this method is supposed to be applied for the case of a complex geometry. This problem can be solved by the R-functions theory, since it allows to construct the necessary sequences of admissible functions in case of the complex domain and different boundary conditions. Note that these admissible functions satisfy exactly the given boundary conditions. As a result, the desired solution is presented in an analytical form. This is a great advantage of this method (RFM) in comparison with other numerical methods. The corresponding set of admissible functions is constructed on the base of the so-called solution structures [33-34]. To use the Rayleigh-Ritz method let us present variational formulation of the given problem. We should find the extremum of the following functional:

$$\pi = U - T, \tag{30}$$

where the strain energy  $U$ , and the kinetic energy  $T$  in the given case are defined by following expressions:

$$U = \int_{\Omega} (N_{11} \varepsilon_{11}^{(0)} + N_{22} \varepsilon_{22}^{(0)} + N_{12} \gamma_{12}^{(0)} + M_{11} \chi_{11} + M_{22} \chi_{22} + M_{12} \chi_{12} + Q_1 \gamma_{13} + Q_2 \gamma_{23}) d\Omega, \tag{31}$$

$$T = \frac{1}{2} \int_{\Omega} \left( I_0 \left( \left( \frac{\partial u_0}{\partial t} \right)^2 + \left( \frac{\partial v_0}{\partial t} \right)^2 + \left( \frac{\partial w_0}{\partial t} \right)^2 \right) + 2I_1 \left( \frac{\partial \psi_x}{\partial t} \frac{\partial u_0}{\partial t} + \frac{\partial \psi_y}{\partial t} \frac{\partial v_0}{\partial t} \right) + I_2 \left( \left( \frac{\partial \psi_x}{\partial t} \right)^2 + \left( \frac{\partial \psi_y}{\partial t} \right)^2 \right) \right) d\Omega. \tag{32}$$

The minimization of functional (30) is performed using the Ritz method. The sequence of coordinate functions in case of the complex planform of the plate is constructed by the R-functions theory [35, 38].



**Table 1.** Comparison of non-dimensional frequencies for square simply supported plate of FGM material  $Al_2O_3/Al$ ,  $p = 2$ ,  $h/2a = 0.1$ .

$\alpha$	Method	1-0-1	1-1-1	1-2-1	2-1-2	2-2-1	2-1-1
P-FGM (imperfect I)							
0	[22]	1.0615	1.1885	1.3024	1.1225	1.2439	1.1653
	RFM	1.0584	1.1857	1.3002	1.1195	1.2415	1.1627
0.1	[22]	0.9826	1.1207	1.2493	1.0471	1.1819	1.0935
	RFM	0.9885	1.1271	1.2549	1.0531	1.1880	1.1007
0.2	[22]	0.8787	1.0420	1.1915	1.9549	1.1105	1.0056
	RFM	0.8913	1.0551	1.2026	0.9684	1.1228	1.0188
P-FGM (imperfect II)							
0.1	[22]	1.0556	1.1708	1.2842	1.1084	1.2270	1.1512
	RFM	1.0565	1.1725	1.2864	1.0941	1.2277	1.1512
0.2	[22]	1.0521	1.1526	1.2658	1.0939	1.2097	1.1376
	RFM	1.0544	1.1581	1.2717	1.0984	1.2126	1.1383
S-FGM (imperfect I)							
0	[22]	1.1617	1.3119	1.4155	1.2427	1.3594	1.2797
	RFM	1.1588	1.3096	1.4137	1.2401	1.3573	1.2774
0.1	[22]	1.1039	1.2595	1.3718	1.1862	1.3113	1.2262
	RFM	1.1105	1.2676	1.3792	1.1942	1.3189	1.2339
0.2	[22]	1.0315	1.2011	1.3256	1.1208	1.2580	1.1632
	RFM	1.0467	1.2173	1.3399	1.1371	1.2732	1.1797
S-FGM (imperfect II)							
0.1	[22]	1.1615	1.2992	1.4001	1.2340	1.3470	1.2712
	RFM	1.1641	1.3029	1.4046	1.2374	1.3502	1.2740
0.2	[22]	1.1620	1.2864	1.3859	1.2255	1.3346	1.2628
	RFM	1.1699	1.2957	1.3948	1.2343	1.3424	1.2702

### 4. Numerical Results

In order to verify the accuracy of the proposed method, we solve the test problem for square simply-supported three-layer plate with side  $2a$ . The bottom and top layers are made of alloy  $Al_2O_3/Al$  and the core is made of ceramics. Thickness of the layers and volume fraction index  $p$  vary. The material properties of the FGM mixture  $Al_2O_3/Al$  are given by [19-23]:

$$\begin{aligned}
 Al: \quad E_m &= 70GPA, & \nu_m &= 0.3, & \rho_m &= 2707kg/m^3, \\
 Al_2O_3: \quad E_c &= 380GPA, & \nu_c &= 0.3, & \rho_c &= 3800kg/m^3.
 \end{aligned}
 \tag{33}$$

The total thickness of the plate is equal to  $h/2a = 0.1$ . The boundary conditions are given by the next formulas:

$$\begin{aligned}
 w = v = \psi_y = N_{11} = M_{11} &= 0 & \text{at } x = \pm a, \\
 w = u = \psi_x = N_{22} = M_{22} &= 0 & \text{at } y = \pm a.
 \end{aligned}$$

This problem has been solved in [22] using a simple higher-order shear deformation theory. Table 1 demonstrates a comparison of the calculated dimensionless frequency:

$$\Lambda = \frac{\lambda(2a)^2}{h} \sqrt{\frac{\rho_0}{E_0}},
 \tag{34}$$

with results reported by [22] in relation with the geometrical ratios  $(h_f - h_c - h_f)$ . In formula (34), it is assumed that  $E_0 = 1 \text{ GPa}$ ,  $\rho_0 = 1 \text{ kg/m}^3$ .

Comparison of data in Table 1 indicates a good agreement between the results obtained and those known in the literature.

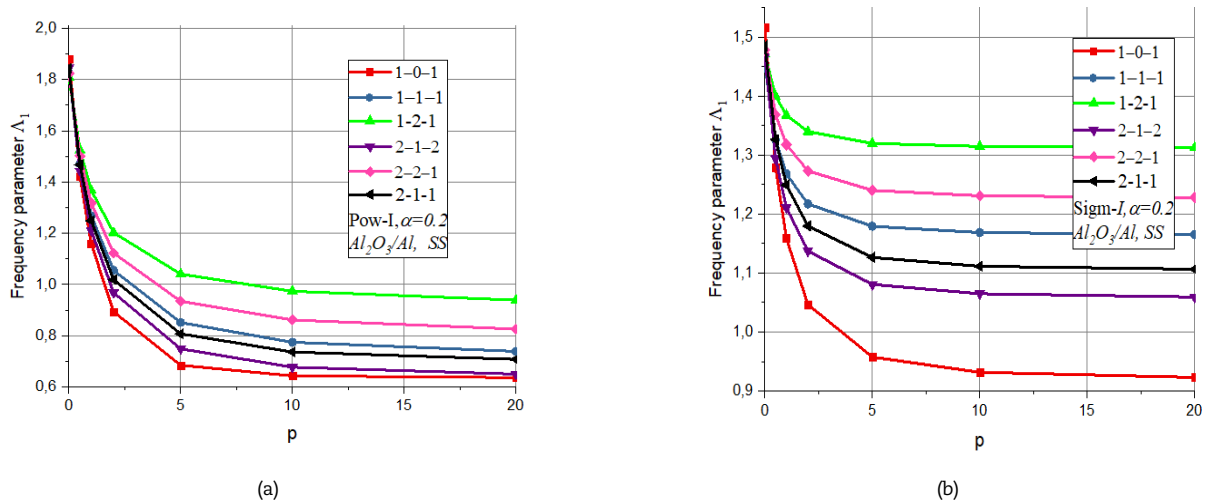


**Fig. 2.** Effect of volume fraction index  $p$  on non-dimensional frequency of FG sandwich simply supported porous plate: (a) P-I; (b) S-I; (c) P-II; (d) S-II.



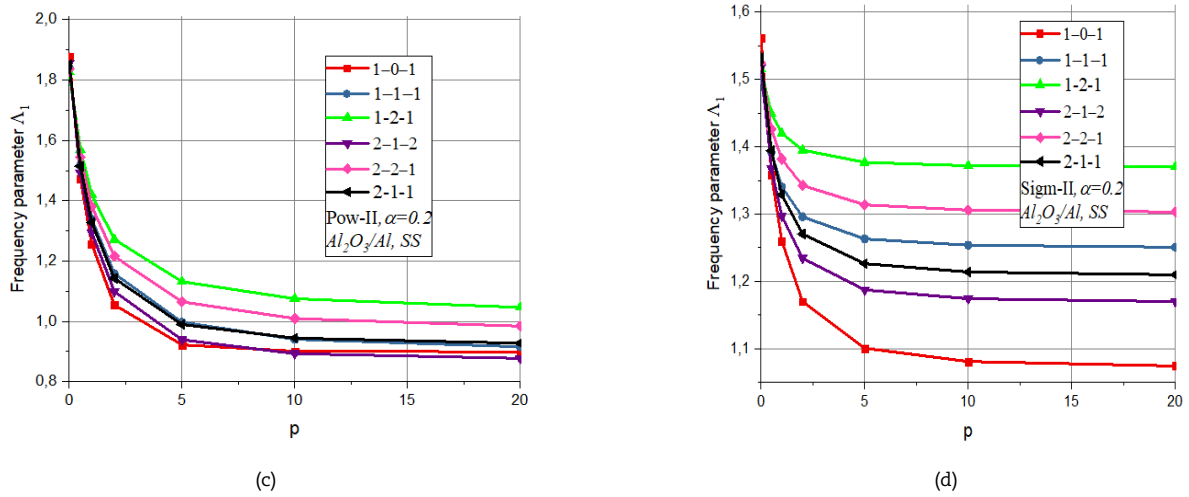


Fig. 2. Continued.

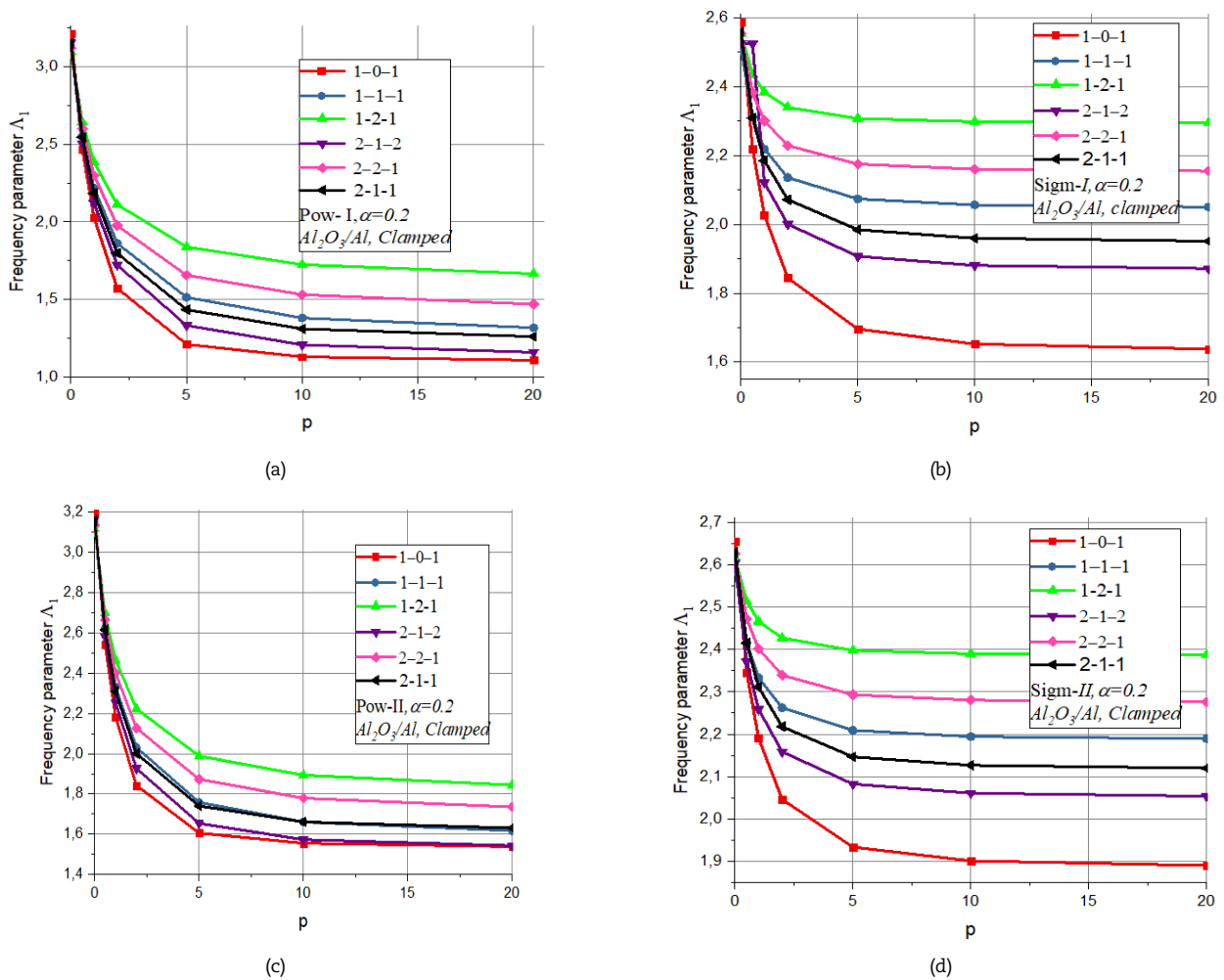


Fig. 3. Effect of volume fraction index  $p$  on non-dimensional frequency of FG porous sandwich clamped square plate: (a) P-I; (b) S-I; (c) P-II; (d) S-II.

Figures 2 and 3 show the influence of the volume fraction index  $p$  on non-dimensional frequency of FG sandwich porous square plate. Results for two models P-FGM and S-FGM for simply supported (SS, Fig. 2a, b, c, d)) and clamped (CL, Fig. 3a, b, c, d) are presented. The porosity coefficient is taken as  $\alpha = 0.2$ . The different lay-up schemes are studied.

It is seen that the frequencies decrease with increasing volume fraction index  $p$  for all cases under consideration because the stiffness of the FG sandwich plate is reduced. The greatest value of the frequencies is observed for lay-up scheme 1-2-1 for two cases of the porosity distribution P-FGM (P-I, P-II) and S-FGM (S-I, S-II) and both the boundary conditions. Obviously, in this case, the proportion of ceramics predominates, and the rigidity of the plate increases. With a uniform distribution of porosity (P-I, S-I), the frequency values are less than with an uneven (P-II, S-II) distribution for all lay-up schemes. This is due to the fact that a large area is occupied by voids with a uniform distribution and the rigidity of the plate decreases.

Let us consider the FG sandwich porous plate with complex planform as shown in Fig. 4.



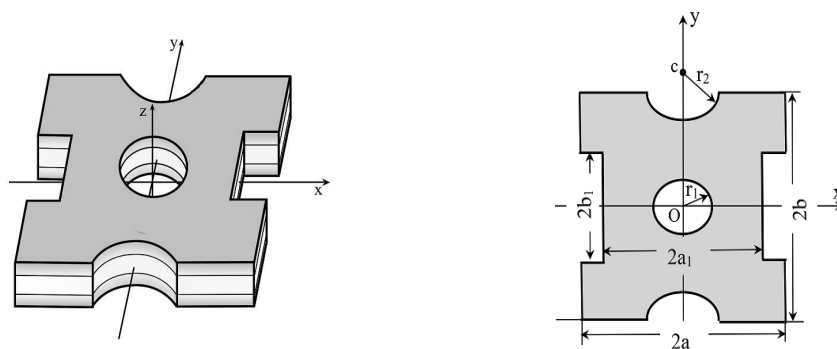


Fig. 4. Sandwich FGM porous plate of complex geometry and its plan form.

Suppose that the plate is clamped along the whole boundary, including the hole. As for the previous problems, it is assumed that the effective properties of FGM to vary through the thickness according to the power and sigmoid laws. Two types of porosity distribution (even and linear-uneven) are considered.

The geometric parameters of the given plate are as follows:

$$\begin{aligned} \frac{h}{2a} &= 0.1; & \frac{b}{a} &= 1; & \frac{a_1}{a} &= 0.45; & \frac{b_1}{a} &= 0.3; \\ \frac{c}{2a} &= 0.7; & \frac{r_1}{2a} &= 0.1; & r_2/2a &= 0.2828. \end{aligned}$$

To use the variational Rayleigh-Ritz method we should construct the sequence of the admissible functions. Applying the R-functions theory [33, 34], first let us construct the corresponding solution structures, which satisfy the given boundary conditions:

$$w(x, y) = 0, \quad u(x, y) = 0, \quad v(x, y) = 0, \quad \psi_x(x, y) = 0, \quad \psi_y(x, y) = 0. \tag{35}$$

Obviously, the solution structures can be taken in the following form:

$$w = \omega\Phi_1, \quad u = \omega\Phi_2, \quad v = \omega\Phi_3, \quad \psi_x = \omega\Phi_4, \quad \psi_y = \omega\Phi_5, \tag{36}$$

where  $\Phi_i, i = \overline{1,5}$  are undetermined components of the solution structures. They are expanded in a power series. In formula (36),  $\omega = 0$  is an equation of the whole border. The function  $\omega(x, y)$  is constructed by the R-functions theory and have the following form:

$$\omega = (f_1 \vee_0 f_2) \wedge_0 (f_3 \wedge_0 (f_4 \wedge_0 f_5)) \wedge_0 (f_6 \wedge f_7).$$

The signs  $\wedge_0$  and  $\vee_0$  define the R-operators: R-conjunction and R-disjunction relatively [33]. Functions  $f_i, i = \overline{1,7}$  are defined as:

$$\begin{aligned} f_1 &= \frac{(a_1^2 - x^2)}{2a_1} \geq 0, & f_2 &= \frac{(b_1^2 - y^2)}{2b_1} \geq 0, & f_3 &= \frac{(x^2 + y^2 - r_1^2)}{2r_1} \geq 0, \\ f_4 &= \frac{(x^2 + (y - b)^2 - r_2^2)}{2r_2} \geq 0, & f_5 &= \frac{(x^2 + (y + b_1)^2 - r_2^2)}{2r_2} \geq 0, \\ f_6 &= \frac{(a^2 - x^2)}{2a} \geq 0, & f_7 &= (b^2 - y^2)/2b \geq 0. \end{aligned}$$

The effect of volume fraction exponent  $p$  on non-dimensional fundamental frequency  $\Lambda = \lambda (2a)^2 \sqrt{\rho_0/E_0}/h$  for FG  $Al_2O_3/Al$  plates with sigmoid porosity distribution is shown in Table 2 (S-I, even case) and Table 3 (S-II, linear- uneven case).

Table 2. Non-dimensional fundamental frequency of vibration of clamped plates with  $h/2a = 0.1, Al_2O_3/Al, \alpha = 0.2$ .

$p$	S-I, $Al_2O_3/Al, \alpha = 0.2$					
	1-0-1	1-1-1	1-2-1	2-1-2	2-2-1	2-1-1
0	9.5334	9.6685	9.8711	9.5975	9.8221	9.7202
0.5	8.6490	9.1495	9.5751	8.9051	9.3755	9.0848
1	8.1282	8.8916	9.4372	8.5368	9.1551	8.7459
2	7.5926	8.6562	9.3167	8.1856	8.9555	8.4223
5	7.1318	8.4750	9.2272	7.9047	8.8028	8.1634
10	6.9918	8.4235	9.2023	7.8230	8.7596	8.0881
20	6.9435	8.4062	9.1940	7.7953	8.7450	8.0625

Table 3. Non-dimensional fundamental frequency of vibration of clamped plates with  $h/2a = 0.1, Al_2O_3/Al, \alpha = 0.2$ .

$p$	S-II, $Al_2O_3/Al, \alpha = 0.2$					
	1-0-1	1-1-1	1-2-1	2-1-2	2-2-1	2-1-1
0	9.7047	9.8532	10.026	9.7862	9.9746	9.8729
0.5	9.0032	9.4182	9.7667	9.2201	9.5948	9.3519
1	8.6111	9.2051	9.6466	8.9278	9.4104	9.0822
2	8.2281	9.0128	9.5421	8.6548	9.2448	8.8296
5	7.9041	8.8663	9.4648	8.4405	9.1193	8.6313
10	7.8094	8.8249	9.4433	8.3789	9.0839	8.5743
20	7.7771	8.8109	9.4361	8.3581	9.072	8.5551





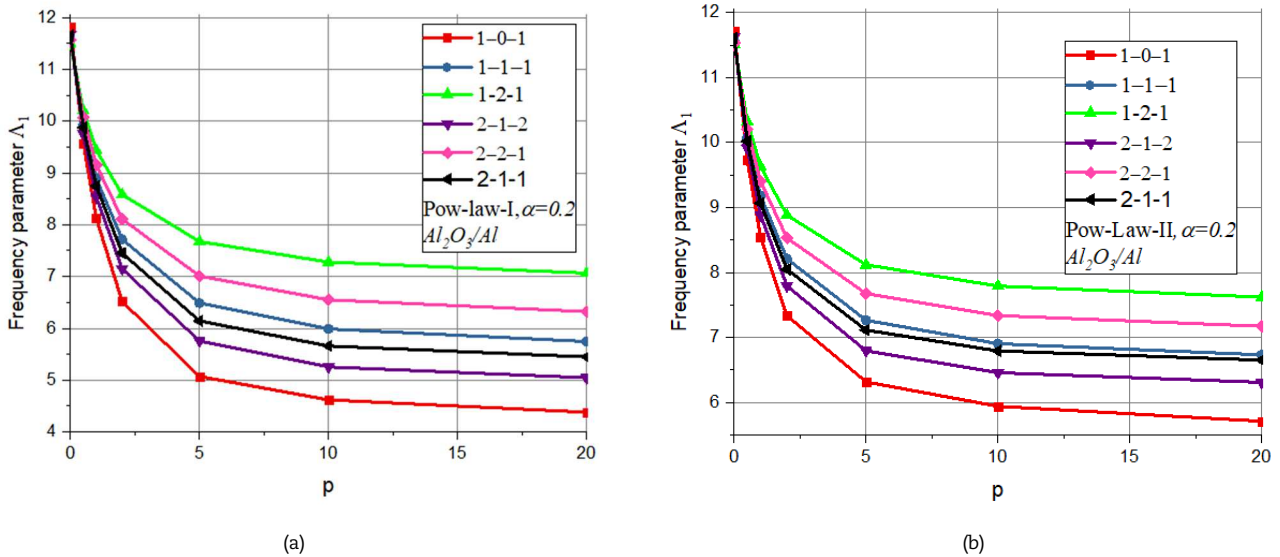


Fig. 5. The variation of the non-dimensional fundamental frequency of FG plate versus power-law index: (a) models P-I; (b) models P-II.

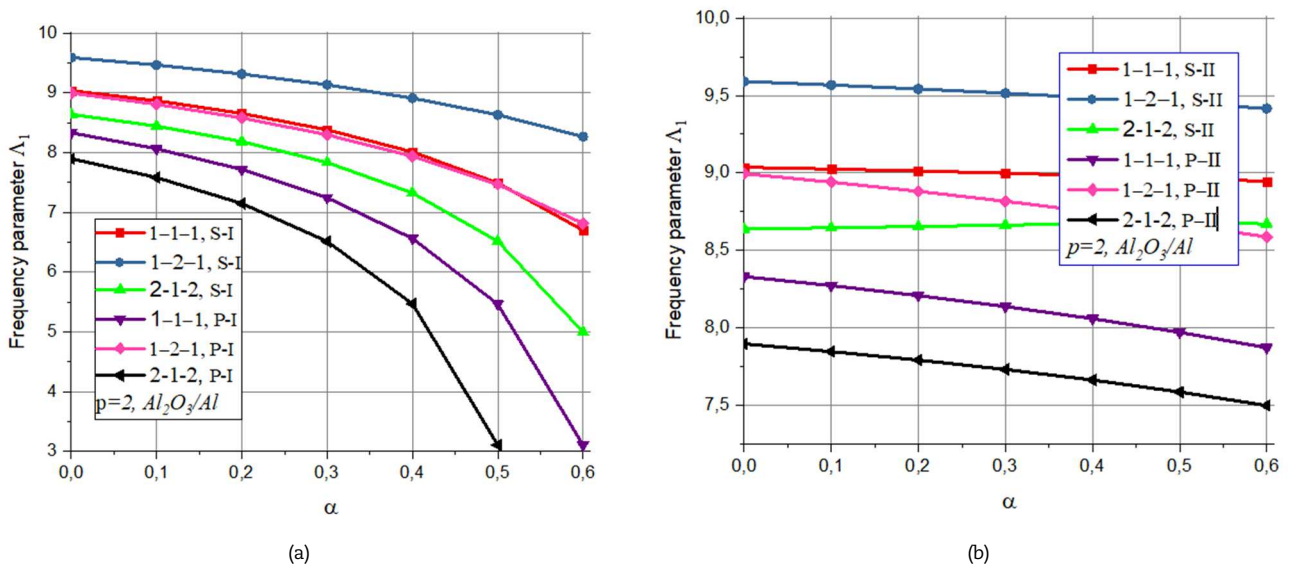


Fig. 6. Effect of the porosity coefficient  $\alpha$  on natural frequencies of the clamped FGM  $Al_2O_3/Al$  sandwich porous plate with complex planform: (a) models P-I, S-I; (b) models P-II, S-II.

Comparison of Table 2 and Table 3 shows that for both types of the sigmoid porosity distribution, the natural frequencies decrease while the power-law index  $p$  increases for the considered lay-up schemes. The non-dimensional frequencies of the plates with lay-up 1-2-1 scheme are greater than corresponding frequencies of the plates with another lay-up schemes in both cases of the porosity distribution. For lay-up scheme 1-0-1, we have values of the non-dimensional frequencies less than those obtained from other lay-up schemes. This is explained by the lower rigidity of the plate with lay-up scheme 1-0-1.

The analogous results for the power-law FG sandwich plates are shown in Fig. 5a (P-I distribution) and Fig. 5b (P-II distribution). Behavior of the FGM sandwich plates for considered law of porosity is similar to S-law of porosity. But the frequencies for the law (P-I, II) porosity distribution are slightly greater than for the sigmoid law (S-I, II).

The variations of non-dimensional frequency for P, S-FGM plate versus parameter porosity  $\alpha$  for clamped porous plate (Fig. 4) made of FGM  $Al_2O_3/Al$  and fixed value of the volume fraction index  $p = 2$  are shown in Fig. 6 (a, b). There are considered the different lay-up schemes of layers (1-1-1; 1-2-1; 2-1-2).

From the illustrated results, it follows that the increase of the porosity coefficient produced the decrease in the frequencies for both laws of the porosity distributions. But in case linear-uneven imperfect FGM sandwich plate (P-II, S-II) this decrease is insignificant.

The effect of different distribution porosities models on natural frequencies is presented in Fig. 6a (models P-I, S-I) and in Fig. 6b (models P-II, S-II). The increase of porosity coefficient  $\alpha$  induces the decrease in the value of natural frequencies for all lay-up schemes of the layers. It is seen that influence of the porosity coefficient  $\alpha$  on frequencies is more significant for an even distribution of porosity than for linear-uneven distribution.

The influence of the porosity coefficient  $\alpha$  on natural frequencies of the plates made of alloy  $Si_3N_4/Sus304$  and  $ZrO_2/Ti-6Al-4V$  with fixed arrangement of layers 2-1-2 and volume fraction index  $p = 2$  is shown in Fig. 7a and Fig. 7b.



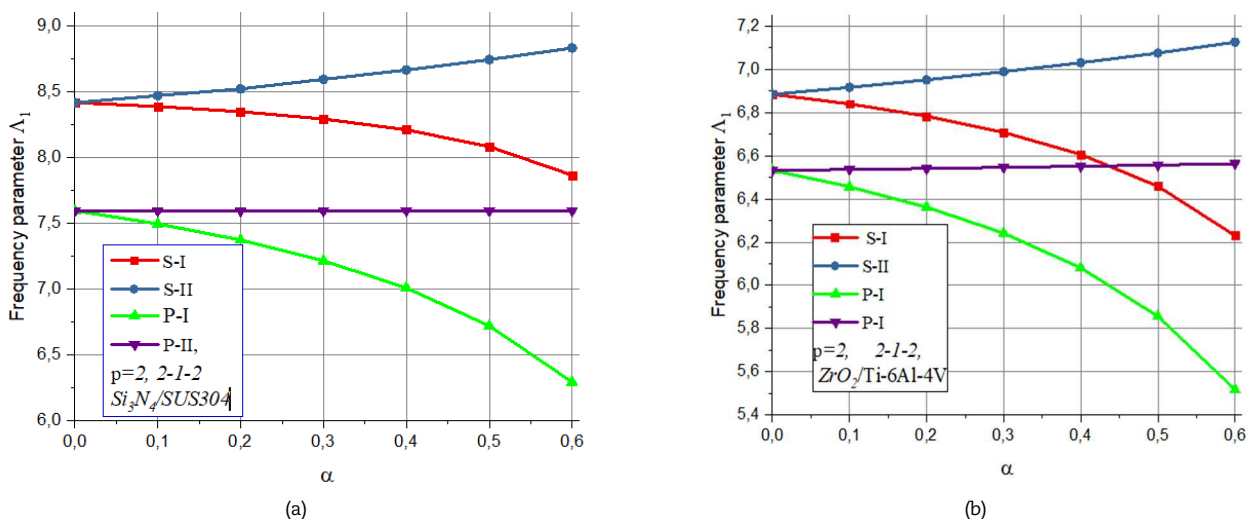


Fig. 7. Effect of the porosity coefficient  $\alpha$  on natural frequencies of the clamped sandwich plate for alloys: (a)  $\text{Si}_3\text{N}_4/\text{SUS304}$ ; (b)  $\text{ZrO}_2/\text{Ti-6Al-4V}$ .

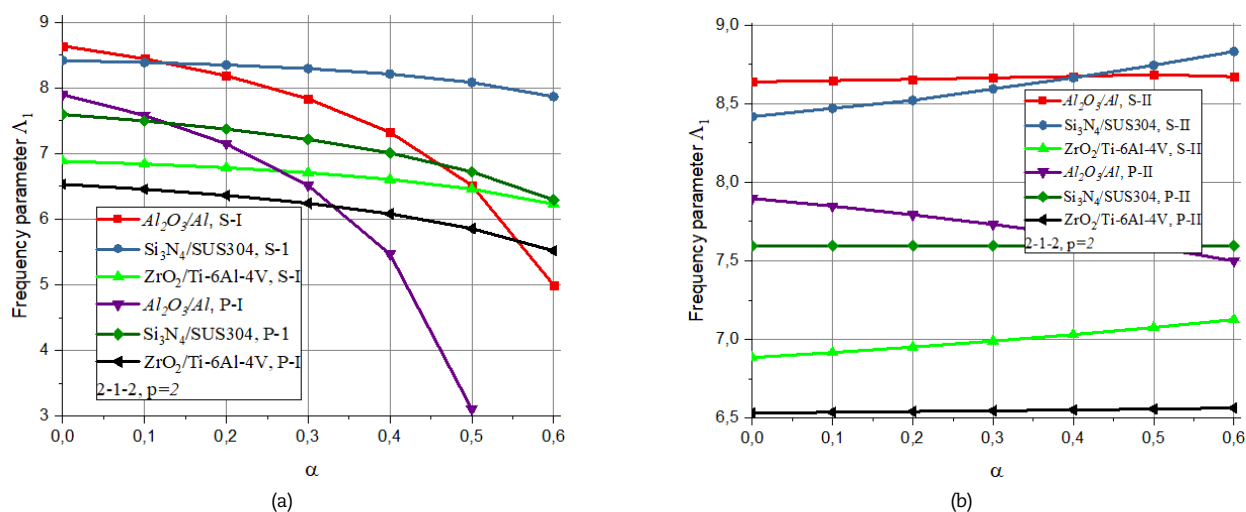


Fig. 8. Comparison of the behavior of the natural frequencies for various types of alloys versus porosity coefficient  $\alpha$ : (a) P-I, S-I; (b) P-II, S-II.

The material properties of these materials were taken as follows [42]:

$$\begin{aligned} \text{Si}_3\text{N}_4: \quad E &= 322.27E_0, \quad \rho = 2370\rho_0; & \text{SUS304}: \quad E &= 207.78E_0, \quad \rho = 8166\rho_0; \\ \text{ZrO}_2: \quad E &= 162E_0, \quad \rho = 3000\rho_0; & \text{Ti-6Al-4V}: \quad E &= 105.69E_0, \quad \rho = 4427\rho_0; \end{aligned}$$

where  $E_0 = 1 \text{ GPa}$ ,  $\rho_0 = 1 \text{ kg/m}^3$ .

Qualitatively, the behavior of natural frequencies with increasing the porosity coefficient  $\alpha$  is the same for both materials. However, the frequency values for alloy  $\text{Si}_3\text{N}_4/\text{SUS304}$  are greater than the corresponding values of the frequencies for alloy  $\text{ZrO}_2/\text{Ti-6Al-4V}$ . It is interesting to note that for both these materials in case of sigmoid linear-uneven porosity model the natural frequencies increase slightly if the porosity coefficient  $\alpha$  decreases.

In Figs. 8a and 8b, the effect of the porosity coefficient  $\alpha$  on natural frequencies of the clamped sandwich plate (2-1-2) for various alloys  $\text{Al}_2\text{O}_3/\text{Al}$ ,  $\text{Si}_3\text{N}_4/\text{SUS304}$  and  $\text{ZrO}_2/\text{Ti-6Al-4V}$  and different porosity models are presented. It should be noted that for all considered FGM materials, the porosity coefficient mainly affects the frequencies for the uniform distribution model for the power-law and sigmoid FGM plate.

### 5. Conclusion

Free vibration analysis of sandwich FGM porous plates with a complex planform was carried out by using the first-order shear deformation theory. The various models for power and sigmoid-law of the porosity distribution were considered and analytical expressions for calculating the components of the stiffness matrix were obtained. The R-functions theory together with the Rayleigh-Ritz method was used for the first time to solve such a class of the problem. Validation of the proposed method was confirmed by comparison of the obtained results for rectangular plates with known ones. New results were obtained for natural frequencies of the clamped porous plate with external cutouts and an internal hole. These results have been carefully studied for various types of FGM materials. The effect of the volume fraction index on natural frequencies was studied for various models of porosity distribution in sandwich plates. The numerical results showed that:

- 1) The natural frequencies decrease if volume fraction index increases for all cases;
- 2) The increase in the porosity coefficient causes the decrease in frequencies for all considered types of FGM and lay-up schemes, except for option S-II (2-1-2). There is a slight increase in frequencies with increasing porosity;
- 3) The effect of the porosity coefficient is more significant for even distribution of plate porosity than for linear-uneven one.



## Author Contributions

L. Kurpa: initiated the research topic and proposed a solution method, and formed the corresponding program. T. Shmatko: derived the formulas for calculating the properties of FGM material and developed the software. J. Awrejcewicz: took part in the discussion on the results and analyzed the verification of the obtained numerical results. G. Timchenko: performed a numerical experiment, testing and verification. I. Morachkovskaya: took part in testing software and verification of the obtained results. The manuscript was written thanks to the contribution of all authors. All authors discussed the results, and checked and approved the final version of the manuscript.

## Acknowledgments

Not Applicable.

## Conflict of Interest

The authors declared no potential conflicts of interest concerning the research, authorship, and publication of this article.

## Funding

The authors received no financial support for the research, authorship, and publication of this article.

## Data Availability Statements

The datasets generated and/or analyzed during the current study are available from the corresponding author on reasonable request.


## References


- [1] Thai, H.-T., Kim, S.-E., A review of theories for the modeling and analysis of functionally graded plates and shells, *Composite Structures*, 128, 2015, 70-86.
- [2] Swaminathan, K., Naveenkumar, D.T., Zenkour, A.M, Carrera, E., Stress, vibration and buckling analyses of FGV plates—A state-of-art review, *Composite Structures*, 120, 2015, 10-31.
- [3] Kumar, Y., The Rayleigh-Ritz method for linear dynamic, static and buckling behavior of beams, shells and plates: A literature review, *Journal of Vibration and Control*, 24(7), 2017, 1-23.
- [4] Sofiyev, A.H., Review of research on the vibration and buckling of the FGM conical shells, *Composite Structure*, 211, 2019, 301-317.
- [5] Malekzadeh, P., Shojaee, M., A unified formulation for free vibration of functionally graded plates, *Journal Science and Engineering of Composite Materials*, 25(1), 2018, 109-122.
- [6] Zenkour, A.M., A comprehensive analysis of functionally graded sandwich plates: Part 2-Buckling and free vibration, *International Journal of Solids and Structures*, 42, 2005, 5243-5258.
- [7] Zenkour, A.M., The refined sinusoidal theory for FGM plates on elastic foundations, *International Journal of Mechanical Sciences*, 51, 2009, 869-880.
- [8] Neves, A.M.A., Ferreira, A.J.M., Carrera, E., Roque, C.M.C., Cinefra, M., Jorge, R.M.N., A quasi-3D sinusoidal shear deformation theory for the static and free vibration analysis of functionally graded plates, *Composites Part B: Engineering*, 2012, 43, 711-725.
- [9] Meiche, N.E., Tounsi, A., Ziane, N., Mechab, I., Bedia, E.A.A., A new hyperbolic shear deformation theory for buckling and vibration of functionally graded sandwich plate, *International Journal of Mechanical Sciences*, 53(4), 2011, 237-247.
- [10] Bessaim, A., Houari, M.S., Tounsi, A., Mahmoud, S.R., Bedia, E.A.A., A new higher-order shear and normal deformation theory for the static and free vibration analysis of sandwich plates with functionally graded isotropic face sheets, *Journal of Sandwich Structures and Materials*, 15(6), 2013, 671-703.
- [11] Meksi, R., Benyoucef, S., Mahmoudi, A., Tounsi, A., Adda Bedia, E.A., Mahmoud, S.R., An analytical solution for bending, buckling and vibration responses of FGM sandwich plates, *Journal of Sandwich Structures and Materials*, 21(2), 2020, 727-757.
- [12] Ton-That, H., A new C0 third-order shear deformation theory for the nonlinear free vibration analysis of stiffened functionally graded plates, *Facta Universitatis-Series Mechanical Engineering*, 19(2), 2021, 285-305.
- [13] Nam, P.V., Kien, N.D., Free vibration of FG sandwich plates partially supported by elastic foundation using a quasi-3D finite element formulation, *Vietnam Journal of Mechanics*, 42(1), 2020, 63-86.
- [14] Nguyen, T.-K., Vo, T.-P., Thai, H.-T., Vibration and buckling analysis of functionally graded sandwich plates with improved transverse shear stiffness based on the first-order shear deformation theory, *Proceedings of the Institution of Mechanical Engineers, Part C: Journal of Mechanical Engineering Science*, 228(12), 2014, 2110-2131.
- [15] Thai, H.T., Nguyen, T.K., Vo, T.P., Lee, J., Analysis of functionally graded sandwich plates using a new first-order shear deformation theory, *European Journal of Mechanics – A/Solids*, 45, 2014, 211-225.
- [16] Thai, H.T., Choi, D.H., A simple first-order shear deformation theory for the bending and free vibration analysis of functionally graded plates, *Composite Structures*, 101, 2013, 332-340.
- [17] Amabili, M., Nonlinear vibrations and stability of laminated shells using a modified first-order shear deformation theory, *European Journal of Mechanics – A/Solids*, 68, 2018, 75-87.
- [18] Tan-Van, V., Ngoc-Hung, N., Khosravifard, A., Hematiyan, M.R., Tanaka, S., Bui, T.Q., A simple FSDT-based meshfree method for analysis of functionally graded plates, *Engineering Analysis with Boundary Elements*, 79, 2017, 1-12.
- [19] Vinh, P.V., Huy, L.Q., Finite element analysis of functionally graded sandwich plates with porosity via new hyperbolic shear deformation theory, *Defence Technology*, 18, 2022, 490-508.
- [20] Shahsavari, D., Shahsavari, M., Li, L., Karami, B., A novel quasi-3D hyperbolic theory for free vibration of FG plates with porosities resting on Winkler/Pasternak/Kerr foundation, *Aerospace Science and Technology*, 72, 2018, 134-149.
- [21] Zenkour, A.M., A quasi-3D refined theory for functionally graded single-layered and sandwich plates with porosities, *Composite Structures*, 201, 2018, 38-48.
- [22] Daikh, A.A., Zenkour A.M., Free vibration and buckling of porous power-law and sigmoid functionally graded sandwich plates using a simple higher-order shear deformation theory, *Materials Research Express*, 6, 2019, 115707.
- [23] Xiang, S., Kang, G-W., Yang, M-S., Zhao, Y., Natural frequencies of sandwich plate with functionally graded face and homogeneous core, *Composite Structures*, 96, 2013, 226-231.
- [24] Gupta, A., Talha, M., Influence of porosity on the flexural and free vibration responses of functionally graded plates in thermal environment, *International Journal of Structural Stability and Dynamics*, 18(1), 2018, 1850013.
- [25] Akbas, S.D., Vibration and static analysis of functionally graded porous plates, *Journal of Applied and Computational Mechanics*, 3(3), 2017, 199-207.
- [26] Wu, D., Liu, A., Huang, Y., Huang, Y., Pi, Y., Gao, W., Dynamic analysis of functionally graded porous structures through finite element analysis, *Engineering Structures*, 165, 2018, 287-301.
- [27] Chen, D., Yang, J., Kitipornchai, S., Buckling and bending analyses of a novel functionally graded porous plate using Chebyshev-Ritz method, *Archives of Civil and Mechanical Engineering*, 19(1), 2019, 157-170.
- [28] Rahmani, M., Mohammadi, Y., Kakavand, F., Vibration analysis of different types of porous FG circular sandwich plates, *International Journal of Advanced Design and Manufacturing Technology*, 12(3), 2019, 63-75.





- [29] Zhang, Y., Jin, G., Chen, M., Ye, T., Yang, C., Yin, Y., Free vibration and damping analysis of porous functionally graded sandwich plates with a viscoelastic core, *Composite Structures*, 244, 2020, 112298.
- [30] Hadji, L., Avcar, M., Free Vibration Analysis of FG Porous Sandwich Plates under Various Boundary Conditions, *Journal of Applied and Computational Mechanics*, 7(2), 2021, 505-519.
- [31] Hadji, L., Avcar, M., Natural frequency analysis of imperfect FG sandwich plates resting on Winkler-Pasternak foundation, *Materials Today: Proceedings*, 53(1), 2022, 153-160.
- [32] Sobhani, E., Avcar, M., Natural frequency analysis of imperfect GNPRN conical shell, cylindrical shell, and annular plate structures resting on Winkler-Pasternak Foundations under arbitrary boundary conditions, *Engineering Analysis with Boundary Elements*, 144, 2022, 145-164.
- [33] Rvachev, V.L., *The R-functions theory and its applications*, Nauk. Dumka, Kiev, 1982 (in Russian).
- [34] Kurpa, L.V., *The R-functions method for solving linear bending and vibration problems of the shallow shells*, NTU "KhPI", Kharkov, 2009 (in Russian).
- [35] Awrejcewicz, J., Kurpa, L., Shmatko, T., Analysis of geometrically nonlinear vibrations of functionally graded shallow shells of a complex shape, *Latin American Journal of Solids and Structures*, 14, 2017, 1648-1668.
- [36] Kurpa, L.V., Shmatko, T.V., Awrejcewicz, J., Linear and nonlinear free vibration analysis of laminated functionally graded shallow shells with complex plan form and different boundary conditions, *International Journal of Non-Linear Mechanics*, 107, 2018, 161-169.
- [37] Kurpa, L.V., Shmatko, T.V., Investigation of free vibrations and stability of functionally graded three-layer plates by using the R-functions theory and variational methods, *Journal of Mathematical Sciences*, 249(3), 2020, 496-520.
- [38] Awrejcewicz, J., Kurpa, L., Shmatko, T., Application of the R-functions in free vibration analysis of FGM plates and shallow shells with temperature dependent properties, *ZAMM Zeitschrift für Angewandte Mathematik und Mechanik*, 101(3), 2021, e20200080.
- [39] Kurpa, L., Shmatko, T., *Parametric vibrations of axially compressed functionally graded sandwich plates with a complex plan form*, In: *Mechanics and Physics of Structured Media*, Academic Press, 2022.
- [40] Shmatko, T., Kurpa, L., Awrejcewicz, J., Dynamic analysis of functionally graded sandwich shells resting on elastic foundations, *Acta Mechanica*, 233, 2022, 1895-1910.
- [41] Kurpa, L., Shmatko, T., Awrejcewicz, J., *Nonlinear Vibration of Functionally Graded Shallow Shells Resting on Elastic Foundations*, In: Lacarbonara, W., Balachandran, B., Leamy, M.J., Ma, J., Tenreiro Machado, J.A., Stepan, G. (eds) *Advances in Nonlinear Dynamics*, NODYCON Conference Proceedings Series, Springer, 2022.
- [42] Kurpa, L., Shmatko, T., Timchenko, G., *Nonlinear Dynamic Analysis of FGM Sandwich Shallow Shells with Variable Thickness of Layers*, *Nonlinear Mechanics of Complex Structures: From Theory to Engineering Applications*, 2021.
- [43] Shen, H.S., *Functionally Graded Materials of Plates and Shells*, CRC Press, Florida, 2009.


## ORCID iD

Lidiya Kurpa  <https://orcid.org/0000-0001-8380-1521>

Tetyana Shmatko  <https://orcid.org/0000-0003-3386-8343>

Jan Awrejcewicz  <https://orcid.org/0000-0003-0387-921X>

Galina Timchenko  <https://orcid.org/0000-0002-7279-7173>

Irina Morachkovskaya  <https://orcid.org/0000-0002-4164-4780>



© 2023 Shahid Chamran University of Ahvaz, Ahvaz, Iran. This article is an open access article distributed under the terms and conditions of the Creative Commons Attribution-NonCommercial 4.0 International (CC BY-NC 4.0 license) (<http://creativecommons.org/licenses/by-nc/4.0/>).

**How to cite this article:** Kurpa L., Shmatko T., Awrejcewicz J., Timchenko G., Morachkovskaya I. Analysis of Free Vibration of Porous Power-law and Sigmoid Functionally Graded Sandwich Plates by the R-functions Method, *J. Appl. Comput. Mech.*, 9(4), 2023, 1144-1155. <https://doi.org/10.22055/jacm.2023.43435.4082>

**Publisher's Note** Shahid Chamran University of Ahvaz remains neutral with regard to jurisdictional claims in published maps and institutional affiliations.

